

# *Characteristics, health risks, and premature mortality attributable to ambient air pollutants in four functional areas in Jining, China*

Article

Published Version

Creative Commons: Attribution 4.0 (CC-BY)

Open Access

Yuan, Y., Zhang, X., Zhao, J., Shen, F., Nie, D., Wang, B. ORCID: <https://orcid.org/0000-0003-1403-1847>, Wang, L., Xing, M. and Hegglin, M. I. ORCID: <https://orcid.org/0000-0003-2820-9044> (2023) Characteristics, health risks, and premature mortality attributable to ambient air pollutants in four functional areas in Jining, China. *Frontiers in Public Health*, 11. 1075262. ISSN 2296-2565 doi: 10.3389/fpubh.2023.1075262 Available at <https://centaur.reading.ac.uk/110740/>

It is advisable to refer to the publisher's version if you intend to cite from the work. See [Guidance on citing](#).

To link to this article DOI: <http://dx.doi.org/10.3389/fpubh.2023.1075262>

Publisher: Frontiers Media

copyright holders. Terms and conditions for use of this material are defined in the [End User Agreement](#).

[www.reading.ac.uk/centaur](http://www.reading.ac.uk/centaur)

## **CentAUR**

Central Archive at the University of Reading

Reading's research outputs online



## OPEN ACCESS

## EDITED BY

Dipesh Rupakheti,  
Nanjing University of Information Science and  
Technology, China

## REVIEWED BY

Kamal Jyoti Maji,  
Georgia Institute of Technology, United States  
Ming Liu,  
Chang'an University, China  
Chao He,  
Yangtze University, China

## \*CORRESPONDENCE

Fuzhen Shen  
✉ f.shen@fz-juelich.de  
Michaela I. Hegglin  
✉ m.i.hegglin@fz-juelich.de

## SPECIALTY SECTION

This article was submitted to  
Environmental Health and Exposome,  
a section of the journal  
Frontiers in Public Health

RECEIVED 20 October 2022

ACCEPTED 03 January 2023

PUBLISHED 19 January 2023

## CITATION

Yuan Y, Zhang X, Zhao J, Shen F, Nie D,  
Wang B, Wang L, Xing M and Hegglin MI (2023)  
Characteristics, health risks, and premature  
mortality attributable to ambient air pollutants  
in four functional areas in Jining, China.  
*Front. Public Health* 11:1075262.  
doi: 10.3389/fpubh.2023.1075262

## COPYRIGHT

© 2023 Yuan, Zhang, Zhao, Shen, Nie, Wang,  
Wang, Xing and Hegglin. This is an open-access  
article distributed under the terms of the  
[Creative Commons Attribution License \(CC BY\)](https://creativecommons.org/licenses/by/4.0/).  
The use, distribution or reproduction in other  
forums is permitted, provided the original  
author(s) and the copyright owner(s) are  
credited and that the original publication in this  
journal is cited, in accordance with accepted  
academic practice. No use, distribution or  
reproduction is permitted which does not  
comply with these terms.

# Characteristics, health risks, and premature mortality attributable to ambient air pollutants in four functional areas in Jining, China

Yue Yuan<sup>1</sup>, Xi Zhang<sup>1</sup>, Jingfeng Zhao<sup>1</sup>, Fuzhen Shen<sup>2,3\*</sup>,  
Dongyang Nie<sup>4</sup>, Bing Wang<sup>5</sup>, Lei Wang<sup>6</sup>, Mengyue Xing<sup>7</sup> and  
Michaela I. Hegglin<sup>2,3\*</sup>

<sup>1</sup>Jining Meteorological Bureau, Shandong, China, <sup>2</sup>Institute of Energy and Climate Research, IEK-7: Stratosphere, Forschungszentrum Jülich, Jülich, Germany, <sup>3</sup>Department of Meteorology, University of Reading, Reading, United Kingdom, <sup>4</sup>School of Environmental Science and Engineering, Southern University of Science and Technology, Shenzhen, China, <sup>5</sup>Henley Business School, University of Reading, Reading, United Kingdom, <sup>6</sup>Jining Bureau of Ecology and Environment, Shandong, China, <sup>7</sup>Business School, Dalian University of Foreign Languages, Liaoning, China

Air pollution is one of the leading causes for global deaths and understanding pollutant emission sources is key to successful mitigation policies. Air quality data in the urban, suburban, industrial, and rural areas (UA, SA, IA, and RA) of Jining, Shandong Province in China, were collected to compare the characteristics and associated health risks. The average concentrations of PM<sub>2.5</sub>, PM<sub>10</sub>, SO<sub>2</sub>, NO<sub>2</sub>, and CO show differences of −3.87, −16.67, −19.24, −15.74, and −8.37% between 2017 and 2018. On the contrary, O<sub>3</sub> concentrations increased by 4.50%. The four functional areas exhibited the same seasonal variations and diurnal patterns in air pollutants, with the highest exposure excess risks (ERs) resulting from O<sub>3</sub>. More frequent ER days occurred within the 25–30°C, but much larger ERs are found within the 0–5°C temperature range, attributed to higher O<sub>3</sub> pollution in summer and more severe PM pollution in winter. The premature deaths attributable to six air pollutants can be calculated in 2017 and 2018, respectively. Investigations on the potential source show that the ER of O<sub>3</sub> (*r* of 0.86) had the tightest association with the total ER. The bivariate polar plots indicated that the highest health-based air quality index (HAQI) in IA influences the HAQI in UA and SA by pollution transport, and thus can be regarded as the major pollutant emission source in Jining. The above results indicate that urgent measures should be taken to reduce O<sub>3</sub> pollution taking into account the characteristics of the prevalent ozone formation regime, especially in IA in Jining.

## KEYWORDS

air pollution, functional regions, health effect, potential source, premature mortality

## 1. Introduction

Air pollution has attracted significant concern worldwide in recent decades, especially in China due to the highest ranking of death records across the world (1). Many previous studies have reported that exposure to both ambient and indoor air pollutants has a direct association with a significantly increased risk of cardiovascular, respiratory, and coronary heart diseases, and even can induce cancer (2–7). Moreover, numerous studies have demonstrated that no matter the long-term or short-term exposure, the varied risk and non-accident premature mortality could be attributed to exposure levels of different air pollutants [i.e., particulate matter with an aerodynamic diameter <2.5 and 10 μm (PM<sub>2.5</sub> and PM<sub>10</sub>), nitrogen dioxide (NO<sub>2</sub>), sulfur dioxide (SO<sub>2</sub>), ozone (O<sub>3</sub>), carbon monoxide (CO)] in one city or at the national scale (8–18).

Health impacts from different air pollutants are usually assessed by epidemiology, toxicology and clinical studies (19, 20). One of the popularly used approaches is the epidemiological statistics method, which can be used to calculate the coefficient of the exposure-response relationship based on the relative mortality risk of air pollutants (21), thus linking pollutants with health risks. At present, many health impact assessment studies have investigated the health risks or premature mortality attributable to a single air pollutant or adjusted for exposure to other pollutants globally or regionally (22–27). In China, numerous epidemiological literature concentrated on the association of single pollutants and population health has been designed by using various methods, which include time-series, cross-sectional, panel, case-crossover, cohort and intervention designs (28). To make an assessment of the short-term health effects of one single air pollutant, time-series studies coupled with Poisson regression or Generalized Additive Model (GAM) were conducted to explore the association of different air pollutants [like NO<sub>2</sub> (29), CO (30), SO<sub>2</sub> (31), PM<sub>10</sub> (32), PM<sub>2.5</sub> (33), and O<sub>3</sub> (34)] and daily mortality in large Chinese cities, including Beijing, Shanghai, Chongqing, Shenyang, and Wuhan (28). Because of the easier conducted research experiment and clearly interpretable result, single-pollutant air quality strategies are widely applicable to protect human health for policy-makers (35). However, the health effect of single-pollutant should be applied cautiously. Because of the certain correlation among different air pollutants, identifying the independent effects of single-pollutant become much more difficult (36). Moreover, the air that humans breathe at once is multiple pollutants. Therefore, exploring the joint effect associated with multi-pollutant should be taken into consideration urgently by scholars.

Currently, three typical approaches, including statistical regression models, the indicator approach, and the source identification methods, can be used to quantify the joint health risk from multi-pollutant (35). Generally, the indicator approach means that it is to use one pollutant to represent the total exposure to several pollutants. To evaluate the total health risks and premature mortalities attributed to different air pollutants (here including PM<sub>2.5</sub>, PM<sub>10</sub>, SO<sub>2</sub>, NO<sub>2</sub>, O<sub>3</sub>, and CO), how to select an appropriate pollutant or construct a health risk index has become more significant. Currently, the air quality is characterized by the widely used Air Quality Index (AQI) system, an index implemented by the central government (like in the US or China) is determined by the primary pollutant rather than the overall air condition (37). To address the inadequacy of the single-pollutant-oriented AQI, the aggregate AQI (AAQI) (38) and air quality health index (AQHI) (39) have been developed and applied in practice. In a recent study, Hu et al. (40) using a novel index referred to as the health risk-based AQI (HAQI), investigated air quality in six representative Chinese cities and found that the total days in a given AQI category (either unhealthy or very unhealthy) were including days in HAQI categories that were equal or even higher than the respective AQI category (i.e., very unhealthy or hazardous). Shen et al. (41) applied the HAQI in 367 cities in China, showing high HAQI to be most prevalent in the North China Plain region (NCP). Zhou et al. (42) established the HAQI in 366 cities in China and found organics were driving PM<sub>2.5</sub>-formation when PM<sub>2.5</sub> is at a lower level of health risk.

Here, we expand on these studies, which focused on atmospheric pollution at the city level (that is averaged over whole cities), to investigate multi-pollutant exposure health risks associated with

different functional areas within a city. To this end, we applied the HAQI calculation to observations obtained from four functional areas in Jining city. Meanwhile, to identify which functional areas and air pollutants play the dominant role in Jining, we introduced the potential source contribution function (PSCF) model in this study as well. The PSCF is a conditional probability model by coupling the pollutant with an air mass arriving at the observational site after having passed through a specific geographical area (43). The PSCF value is determined by dividing the space up into certain grid cells and checking the back-trajectory endpoint to see if there was a sampling day commensurate with the trajectory. The PSCF analysis is widely applied to identify the potential source of any pollutant, like SO<sub>2</sub> (44), NO<sub>2</sub> (45), PM<sub>2.5</sub> (46), PM<sub>10</sub> (47), CO (48), and O<sub>3</sub> (48) black carbon particles (49), or a pollutant-related indicator (e.g., excess risk in section 2.4) (41).

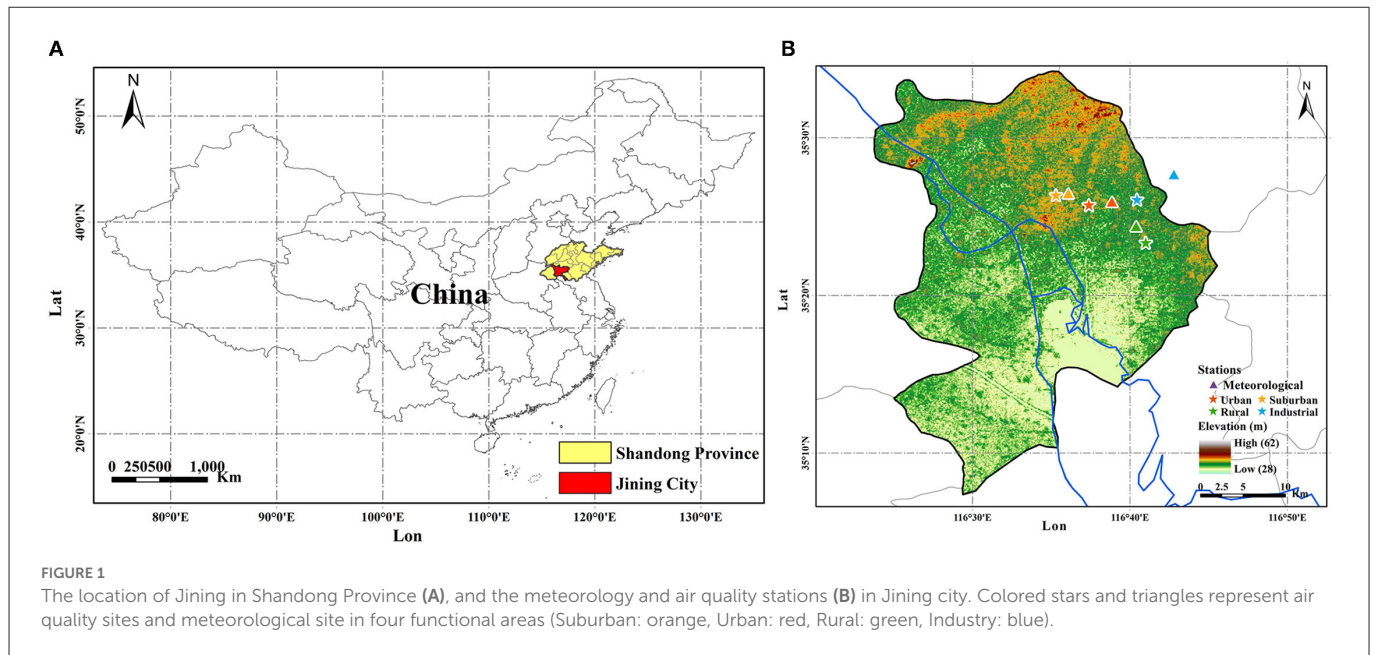
At last, the results aim at providing a clear understanding of the regional distribution of health risks and to provide guidance to policy-makers for effective mitigation policies within Jining's city borders. In particular, Jining is located between the Beijing-Tianjin-Hebei region and the Yangtze River Delta, which is prone to air pollution under a zonal circulation and stable synoptic conditions (low wind and high relative humidity) aside from strong emissions of pollutants, especially in winter and spring. To evaluate the air quality expected over the 2017–2018 period and the associated feedback on health risks in four different functional regions in Jining city, this study aims to: (1) compare the air pollution levels across the four functional areas; (2) estimate the multi-pollutant exposure health risk in these functional areas; (3) evaluate all-cause premature mortalities attributable to all air pollutants, and (4) identify which functional areas and air pollutants are the major contributors to the health risk of Jining City.

## 2. Materials and methods

### 2.1. Site and data

The study region, Jining (116°26'–116°44' E, 35°08'–35°32' N), is located in the southwest of Shandong Province in eastern China (Figure 1A). The air sampling sites (colored stars) and meteorological stations (colored triangles) are located in the four different functional areas identified in Jining. Highways and industrial parks are found near the industrial (IA) site. For the urban (UA) site in the city center, the nearby road network is complex, with heavy traffic and high building density. The suburban (SA) site is located between the urban and rural areas, and the rural (RA) site is located by a farm and river and far away from the city center. The surrounding environment of each air quality sampling site is largely consistent with the basic characteristics of the functional areas. The meteorological stations were chosen to be as close as possible to the air pollutant sampling sites.

The hourly monitoring data of six pollutants and the hourly meteorological data at each site were obtained from the website of the Environmental Meteorological Platform of Shandong (<http://10.76.10.119/>) and the Jining Meteorological Bureau, respectively. The meteorology factors include temperature (°C), wind direction (WD), and wind speed (WS). Here, WS and WD were used to explore the potential source region of pollution. The temperature



was applied to investigate the impact on air pollutants, especially for O<sub>3</sub>. Based on the daily minimum requirement for the validity of air pollutant concentration data (Chinese Ambient Air Quality Standard GB 3095-2012) ([https://www.mee.gov.cn/ywgz/fgbz/bz/bzwb/dqjhjzlbz/201203/t20120302\\_224165.shtml](https://www.mee.gov.cn/ywgz/fgbz/bz/bzwb/dqjhjzlbz/201203/t20120302_224165.shtml)), the daily and monthly data during 2017 (2018) reported in this study are valid for 362 (365) days and 12 (12) months, respectively. The other days in 1 year were deleted due to the sampling data being <20 h in a day. For the meteorology dataset, all the data used each day is valid according to China's Surface Meteorological Observation Standard (CSMOS) ([https://www.cma.gov.cn/zfxgk/gknr/flfgbz/bz/202209/t20220921\\_5099079.html](https://www.cma.gov.cn/zfxgk/gknr/flfgbz/bz/202209/t20220921_5099079.html)). For precipitation and relative humidity, we did not explore the impact of the two meteorology factors on air pollution due to the large number of missing values.

## 2.2. The calculation method of excess risk and health-risk based AQI

The relative risk (RR) of each pollutant is expressed by an exponential-linear function as shown in Eq. 1 (40). Here,  $\beta_i$  is the exposure-response relationship coefficient (which quantifies the additional health risk per unit increase of an air pollutant) with values of 0.038, 0.032, 0.081, 0.13, and 0.048% per  $\mu\text{g}/\text{m}^3$  for PM<sub>2.5</sub>, PM<sub>10</sub>, SO<sub>2</sub>, NO<sub>2</sub>, and O<sub>3</sub>, respectively, and 3.7% per  $\text{mg}/\text{m}^3$  for CO (50).  $C_i$  represents the mass concentration of a pollutant  $i$ . Meanwhile, a baseline concentration  $C_{i,0}$  is also defined to determine the minimum risk of each pollutant  $i$ , meaning one pollutant has no health risk when its concentration is below or equal to  $C_0$ , that is,  $RR_i = 1$ . Here, the upper threshold values of Chinese Ambient Air Quality Standard (CAAQS) 24-h Grade II were regarded as the  $C_{i,0}$  (Supplementary Table 1). The excess risk (ER) of pollutant  $i$  is written as in Eq. 2 and the total ER can be calculated by adding up the ER of each pollutant (Eq. 3). It should be noted that the ER added up linearly could over-estimate the assessment of total ER if those pollutants are highly correlated. Therefore, the total ER from six air

pollutants can be regarded as an upper-bound estimation (40).

$$RR_i = \exp[\beta_i (C_i - C_{i,0})], \quad C_i > C_{i,0} \quad (1)$$

$$ER_i = RR_i - 1 \quad (2)$$

$$ER_{total} = \sum_{i=1}^n ER_i = \sum_{i=1}^n (RR_i - 1). \quad (3)$$

After calculating the total ER, the combined multi-pollutant Relative Risk ( $RR^*$ ) and an equivalent total concentration ( $C_i^*$ ) of pollutant  $i$  (40) can be written as:

$$RR^* = ER_{total} + 1 = \exp[\beta (C^* - C_0)] \quad (4)$$

$$C_i^* = \frac{\ln(RR^*)}{\beta_i + C_{0,i}} \quad (5)$$

Finally,  $C_i^*$  is substituted for the  $C_{i,m}$  in the AQI calculation to yield the HAQI (40), where the AQI calculation is as follows:

$$AQI_i = \frac{AQI_{ij} - AQI_{i,j-1}}{(C_{i,j} - C_{i,j-1})} \times (C_{i,m} - C_{i,j-1}) + AQI_{i,j-1}, \quad j > 1 \quad (6)$$

$$AQI_i = AQI_{i,1} \frac{C_{i,m}}{C_{i,1}}, \quad j = 1 \quad (7)$$

$$AQI = \max(AQI_1, AQI_2, \dots, AQI_n), \quad n = 1, 2, \dots, 6. \quad (8)$$

where  $C_{i,m}$  is the measured concentration of pollutant  $i$ ;  $j$  is the health category index;  $C_{i,j}$  is the reference concentration for pollution



$i$  corresponding to the  $j$ -th health category. Accordingly, the HAQI calculation could be demonstrated as follows:

$$HAQI_i = \frac{HAQI_{ij} - HAQI_{ij-1}}{(C_{ij} - C_{ij-1})} \times (C_i^* - C_{ij-1}) + HAQI_{ij-1}, j > 1, \quad (9)$$

$$HAQI_i = HAQI_{i,1} \frac{C_i^*}{C_{i,1}}, j = 1 \quad (10)$$

$$HAQI = \max(HAQI_1, HAQI_2, \dots, HAQI_n), n = 1, 2, \dots, 6. \quad (11)$$

## 2.3. Daily cause-specific mortality and health burden assessment

The annual all-cause mortality in Jining was obtained from the Jining Statistical Yearbooks 2017 and 2018. The daily mortality was then calculated by the annual mortality rate divided by the number of days per year. The estimated health burden owing to short-term exposure to air pollutants can be calculated as follows (51, 52):

$$M = \sum_i^n AF_i \times BM \quad (12)$$

$$AF_i = (RR_i - 1) / RR_i \quad (13)$$

where  $M$  (total mortality due to atmospheric pollution),  $n$  (total number of days),  $BM$  (daily baseline mortality),  $AF_i$  (daily attributable fraction related to short-term exposure of air pollutant  $i$ ).

## 2.4. Potential source contribution function analysis

In this study, back trajectory analyses were performed by using the Hybrid Single-Particle Lagrangian Integrated Trajectory HYSPLIT model (Version 4.9) (53). The 72 h back trajectories arriving at Jining city at a height of 300 m were calculated every 3-h from 2017 to 2018. Based on these back trajectories data, a potential source contribution function (PSCF) analysis (54) was executed with ZeFir, an Igor-based (Wavemetrics, USA) package (55). PSCF analyses are commonly used to investigate the origin of observed concentrations at a sampling site under a given criterion (here, the 75th percentile value).

$$PSCF_{i,j} = \frac{m_{i,j}}{n_{i,j}} \quad (14)$$

where  $n_{i,j}$  and  $m_{i,j}$  are the total count of endpoints and above-threshold endpoints located in the  $i$ ,  $j$ th air cell, respectively. A sigmoid weighting function (41) was used to reduce the influence of large differences between two air cells (see Eq. 15). Three values in this function are 10, 0.5, 0.1 for  $a$ ,  $b$ ,  $c$  respectively (41). It is written as follows:

$$W = \frac{1}{(1+c)(1+e^{-a(x-b)})} + \frac{c}{1+c} \quad (15)$$

$$x = \log(n_{i,j} + 1) / \max_{\log(n_{i,j} + 1)} \quad (16)$$

After calculating the PSCF for each sampling site in one city individually, the combined PSCF over all the sampling sites in the city can be calculated by using a multi-site (MS) merging method:

$$MS_{i,j} = \frac{\sum_l m_{i,j}^l}{\sum_l n_{i,j}^l} \quad (17)$$

where  $m^l$  and  $n^l$  values indicate the  $m$  and  $n$  number counts of the sampling sites  $l$  in Jining.

## 3. Results and discussion

### 3.1. Comparison of six pollutants in four functional areas

Figure 2 shows the annual mean mass concentrations of six pollutants in Jining during 2017 and 2018 at the city level.  $PM_{2.5}$ ,  $PM_{10}$ ,  $SO_2$ ,  $NO_2$ , and  $CO$  all show lower values in 2018 than in 2017, indicating decreased emissions between the 2 years with 3.87% (from 57.11 to 54.89  $\mu\text{g}/\text{m}^3$ ), 16.67% (from 107.65 to 89.71  $\mu\text{g}/\text{m}^3$ ), 19.24% (from 26.27 to 21.21  $\mu\text{g}/\text{m}^3$ ), 15.74% (from 40.97 to 34.52  $\mu\text{g}/\text{m}^3$ ) and 8.37% (from 10.43 to 9.56  $\text{mg}/\text{m}^3$ ), respectively. Conversely, the mass concentration of  $O_3$  was elevated by 4.5% (from 99.26  $\mu\text{g}/\text{m}^3$  to 103.72  $\mu\text{g}/\text{m}^3$ ). Elevated  $O_3$  mass concentrations and decreased mass loadings of PM have become a generally observed phenomenon resulting from pollution control measures, indicating that fewer PM but more  $O_3$  pollution events may also occur in Jining city in the future. Following many previous studies reports (56–59), this finding also stresses the key role of controlling  $O_3$  pollution through a series of strategies, such as the reduction of anthropogenic emissions, adjustment of the temperature, and balanced  $NO_x$  and VOC control, for the local government in the future.

The seasonal distributions of the six pollutants averaged over the 2 years were then compared among four functional areas: UA, SA, RA, and IA, with the results shown in Figure 3A. Overall, the mass loading of all pollutants (except for  $O_3$ ) exhibited high (low) mass concentrations in winter and low (high) mass concentrations in summer. The seasonal patterns of all the air pollutants' mass loadings in Jining are consistent with that in almost all other cities across China (41, 42). The higher concentrations of the six air pollutants, except for ozone, in winter, can be explained by enhanced coal combustion, biomass burning, and unfavorable meteorological conditions, including low temperature (2.6°C), and boundary layer height (395 m) in winter (Supplementary Figure 1). The opposite behavior of the ozone concentrations, with the highest values during spring/summer is a well-known consequence of photochemistry, which is most active in these seasons.

After identifying the seasonal patterns of the six air pollutants in the four functional areas, the differences in the annual mean behavior (averaged over 2017 and 2018) of the mass loadings of the six air pollutants among UA, SA, RA, and IA are discussed. For PM ( $PM_{10}$  and  $PM_{2.5}$ ), the order of mass loading from high to low follows as: IA (105.00 and 60.37  $\mu\text{g}/\text{m}^3$ ) > RA (103.57 and 57.56  $\mu\text{g}/\text{m}^3$ ) > UA (98.52 and 54.49  $\mu\text{g}/\text{m}^3$ ) > SA (88.61 and 53.26  $\mu\text{g}/\text{m}^3$ ). With the contribution of fossil fuel combustion from plenty of power plants and the emissions from factories in this area, the IA had a higher

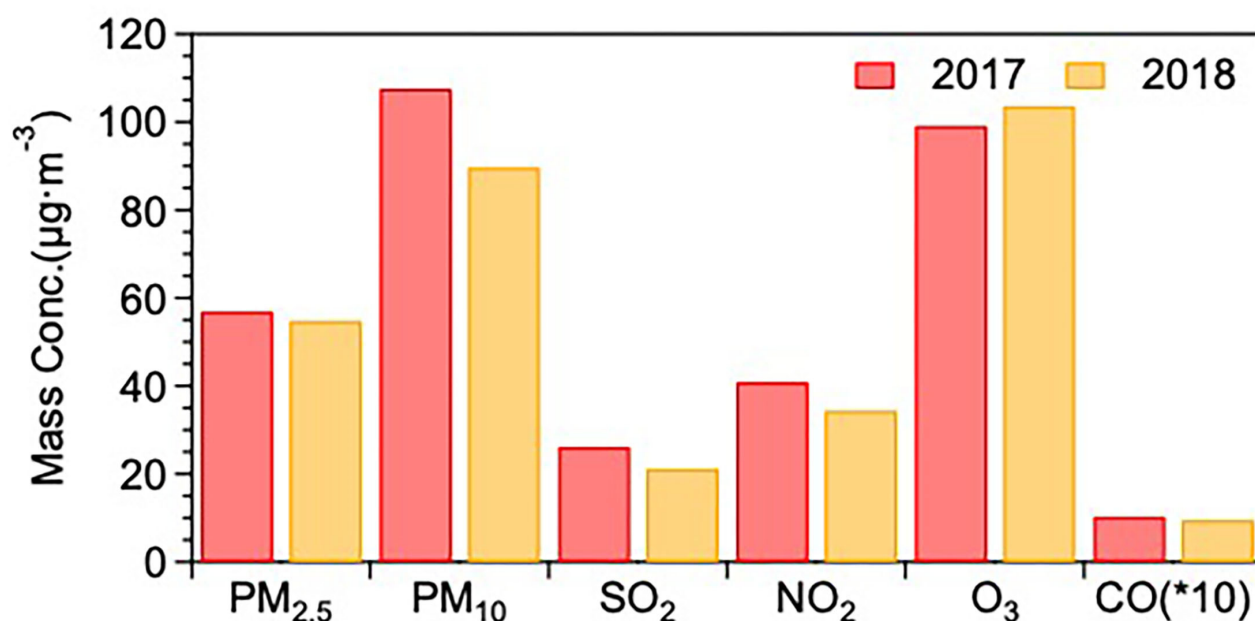


FIGURE 2

The annual mean mass concentrations of six pollutants in Jining during 2017 and 2018 [the unit of CO is  $\text{mg}/\text{m}^3$ , CO (\*10) means the real CO mass concentration multiple 10].

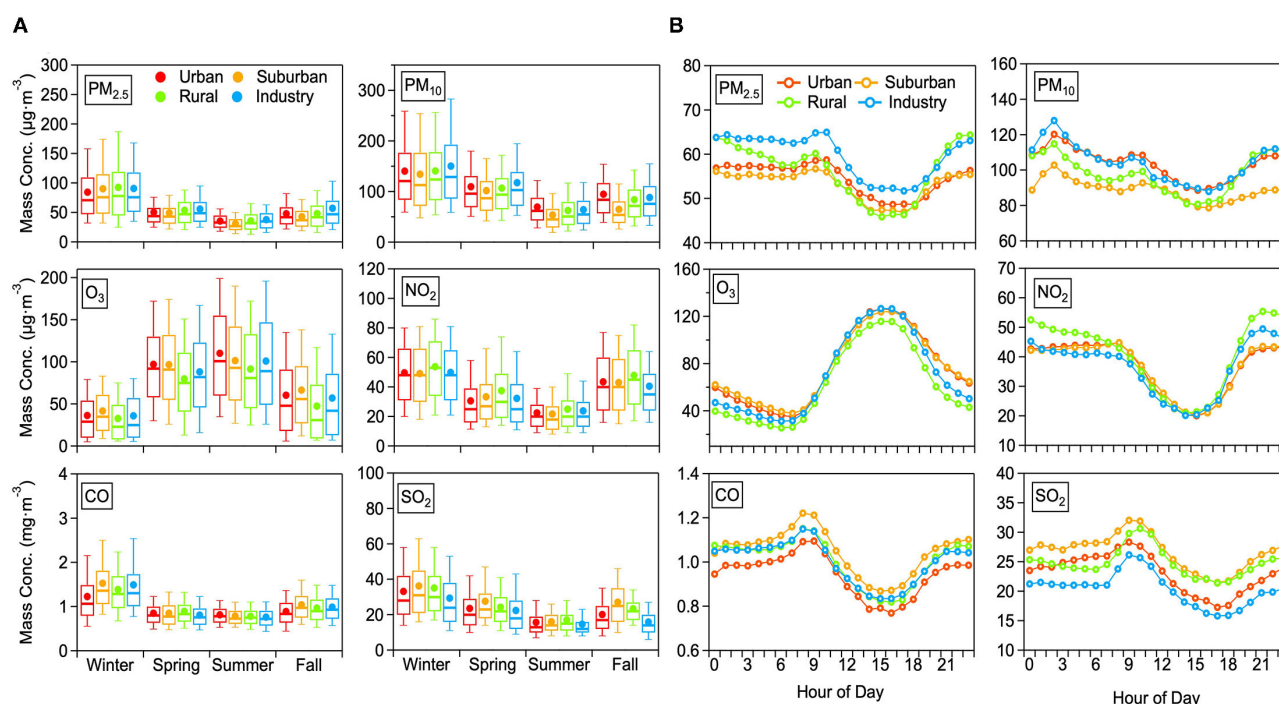


FIGURE 3

The seasonal (A) and diurnal (B) distributions of the six pollutants averaged over 2017 and 2018 for each of the functional areas (color-coded).

mass concentration of PM than in the other three areas in all four seasons (except for the  $\text{PM}_{10}$  in summer and fall). The local source of high mass loading of PM in RA results mainly from residents cooking and straw burning. The higher  $\text{PM}_{10}$  in UA compared to that in IA in summer and fall might be ascribed to the heavy traffic

emissions and unfavorable pollution dilution conditions due to high building density. For  $\text{NO}_2$  and  $\text{SO}_2$ , the mass concentrations in these areas followed the order of RA ( $41.02 \mu\text{g}/\text{m}^3$ ) > UA ( $36.79 \mu\text{g}/\text{m}^3$ ) > IA ( $36.61 \mu\text{g}/\text{m}^3$ ) > SA ( $36.52 \mu\text{g}/\text{m}^3$ ) and SA ( $26.74 \mu\text{g}/\text{m}^3$ ) > RA ( $24.92 \mu\text{g}/\text{m}^3$ ) > UA ( $23.13 \mu\text{g}/\text{m}^3$ ) > IA ( $20.56 \mu\text{g}/\text{m}^3$ ),

respectively. The mass concentrations of NO<sub>2</sub> and SO<sub>2</sub> were the highest in IA and SA, respectively. For CO, the mass loading was very similar during spring, summer, and fall. In winter, on the other side, the concentrations were decreasing following the order of SA (1.53 mg/m<sup>3</sup>) > IA (1.49 mg/m<sup>3</sup>) > RA (1.38 mg/m<sup>3</sup>) > UA (1.23 mg/m<sup>3</sup>). The SA and IA sites are located at the edge of the city and nearby the outside ring of a highway, therefore, higher traffic emissions of CO might be the main source in SA and IA. At last, for O<sub>3</sub>, the mass loading ranked from high to low as: SA (76.61 μg/m<sup>3</sup>) ≈ UA (76.00 μg/m<sup>3</sup>) > IA (70.49 μg/m<sup>3</sup>) > RA (62.88 μg/m<sup>3</sup>). Even though the average mass loading of O<sub>3</sub> in SA was almost equal to that in UA in all four seasons, the O<sub>3</sub> in UA was significantly higher than that in SA in summer, indicating a phenomenon that O<sub>3</sub> pollution has become an increasing concern for the urban residents in Jining. On the other hand, O<sub>3</sub> in RA was the lowest in all seasons.

Figure 3B illustrates the diurnal pattern of the six standard pollutants in the four functional areas. The different functional areas exhibit very similar diurnal cycles for the same pollutant. Overall, the mass loadings of PM<sub>2.5</sub> and NO<sub>2</sub> during night-time were stable but started to drop after 9:00 a.m. After reaching minimum values around 4:00 p.m., they began to increase until 11:00 p.m. For PM<sub>10</sub>, the diurnal pattern is different to PM<sub>2.5</sub> and exhibits two peaks at 3:00 a.m. and 9:00 a.m. and a valley at 4:00 p.m. Overall, PM and NO<sub>2</sub> concentrations during night-time surpass daytime values and an obvious decrease appears in the afternoon, which could be interpreted by the strengthened emission (traffic emission, resident heating, etc.) during night-time and an elevated height of the planetary boundary layer (PBL) during the afternoon. Meanwhile, the decreased concentrations of gas pollutants, including SO<sub>2</sub> and CO, in the afternoon also can be explained by the increased height of PBL, which can dilute those gas pollutants. However, morning peaks (at 9:00 am) of PM, SO<sub>2</sub> and CO can be attributed to enhanced fossil fuel combustion.

### 3.2. Health risk in four functional areas

In the next step, the average AQI and HAQI values were calculated over the 2017–2018 time period based on the daily average values of pollutants (Figure 4). In the four functional areas, the mean value of AQI and HAQI in 2017–2018 decreases following the order: IA (AQI: 106.9 ± 47.0, HAQI: 121.3 ± 71.5) > UA (AQI: 103.6 ± 45.2, HAQI: 117.0 ± 68.2) > SA (AQI: 101.5 ± 47.1, HAQI: 112.5 ± 68.0) > RA (AQI: 99.1 ± 46.1, HAQI: 108.8 ± 65.0). For all functional areas, the mean values of HAQI are higher than the AQI value, which is consistent with the finding of studies concentrated on the comparison between AQI and HAQI (21, 40, 42). The main reason for higher HAQI than AQI is that the HAQI reflects comprehensive health risk rather than the single-pollutant oriented AQI.

It is interesting to also look at the total ERs needed as input to the HAQI calculation and which were calculated by using Eq. 3. It should be noted that SO<sub>2</sub> and CO concentrations were always below the threshold concentration and thus the two pollutants had no exposure health risk to the public people. The total ER in IA (Figure 5) was the highest with a value of 2.38%, followed by 2.35% in UA, 1.50% in SA, and 1.20% in RA, respectively. For total ERs in the four functional areas, ERs of O<sub>3</sub> (IA: 0.88%, UA: 1.05%, SA: 0.89%, RA: 0.41%) made the dominant contribution to total ERs. For the total ER in IA, the

ER of PM<sub>2.5</sub> and PM<sub>10</sub> made an almost equal contribution (0.71% and 0.72%) after that of O<sub>3</sub>, followed by the contribution of NO<sub>2</sub> (0.06%). In UA, the other total ER contributors amounted to 0.58% for PM<sub>2.5</sub>, 0.68% for PM<sub>10</sub>, and 0.04% for NO<sub>2</sub>. In SA, the other three contributions to the total ER were 0.30% for PM<sub>2.5</sub>, 0.24% for PM<sub>10</sub>, and 0.07% for NO<sub>2</sub>, respectively. Except for the ER of O<sub>3</sub>, the ER of PM<sub>2.5</sub>, PM<sub>10</sub>, and NO<sub>2</sub> in RA were 0.29, 0.26, and 0.24%, respectively. For total ERs in RA, even though the major contributor of O<sub>3</sub> is rather low compared to the other functional areas, the highest ER for NO<sub>2</sub> can offset the contribution from O<sub>3</sub>, leading to the not quite low HAQI in RA.

### 3.3. Premature mortality attributable to air pollutants

After evaluating the total ERs from six air pollutants in Jining, we can further investigate the premature mortality attributable to different air pollutants. Based on monitoring data of six pollutants in 2017 and 2018, the all-cause premature mortality by short-term exposure to air pollution in Jining was calculated here. The total premature mortality caused by air pollution for the 2 years was 6,072 and 2,145 for 2017 and 2018, respectively (Table 1). Specifically, the premature mortalities attributable to NO<sub>2</sub>, O<sub>3</sub>, PM<sub>10</sub>, and PM<sub>2.5</sub> were 912, 1,755, 1,824, 1,581 for 2017 and 175, 666, 593, and 710 for 2018. For the number of premature mortality attributable to PM<sub>2.5</sub> in 2017, it is almost consistent with the death number of 1,488 in terms of the total population (1.5 million) (60). PM<sub>10</sub> was the dominant contributor to premature deaths in 2017, but its contribution decreased from 30.0% in 2017 to 27.7% in 2018. The relative contribution of O<sub>3</sub> increased from 28.9% in 2017 to 31.0% in 2018, exceeding the relative contribution of PM<sub>10</sub> in 2018. The changing contributions of PM<sub>10</sub> and O<sub>3</sub> to the total premature mortality between 2017 and 2018 are directly related to the opposed changes in their observed concentrations. Furthermore, the contribution of NO<sub>2</sub> decreased from 15.0% in 2017 to 8.2% in 2018. Note, the health effects of SO<sub>2</sub> and CO are not shown in the table because their concentrations are always under the threshold values and thus do not contribute to premature mortality.

Looking into the four functional areas separately, the number of NO<sub>2</sub>-driven premature deaths in RA and IA was higher in 2017 than that in 2018, and their relative contributions decreased from 22.9% and 24.9% in 2017 to 7.2% and 15.8% in 2018, respectively. Note, the contribution of NO<sub>2</sub> to premature death was much lower and the inter-annual variation was not significant in the other two regions. Inspection of the contribution of O<sub>3</sub> to premature death in UA and SA reveals its significance in these areas, notably increasing from 43.5 and 40.1% in 2017 to 48.31 and 47.83% in 2018, respectively, and representing the main factor leading to premature death in UA and SA. In the other two regions, the contribution of O<sub>3</sub> to premature death was relatively low and the inter-annual variation was not significant.

The contributions of PM<sub>10</sub> and PM<sub>2.5</sub> to premature death in the four regions varied between 2017 and 2018. In RA, the contribution rates of PM<sub>10</sub> and PM<sub>2.5</sub> increased from 30.9 and 29.3% in 2017 to 38.2 and 42.8% in 2018, respectively. In SA



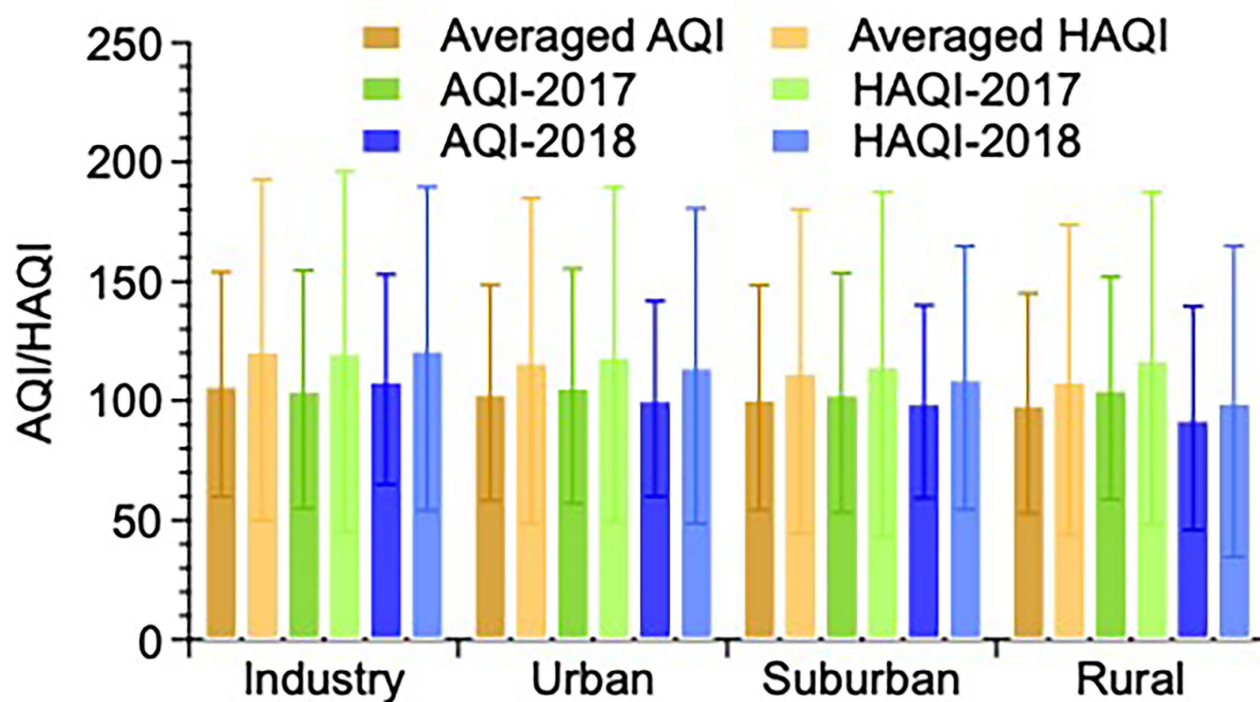


FIGURE 4  
The mean AQI and HAQI average over 2017 and 2018 in four functional areas in Jinan.

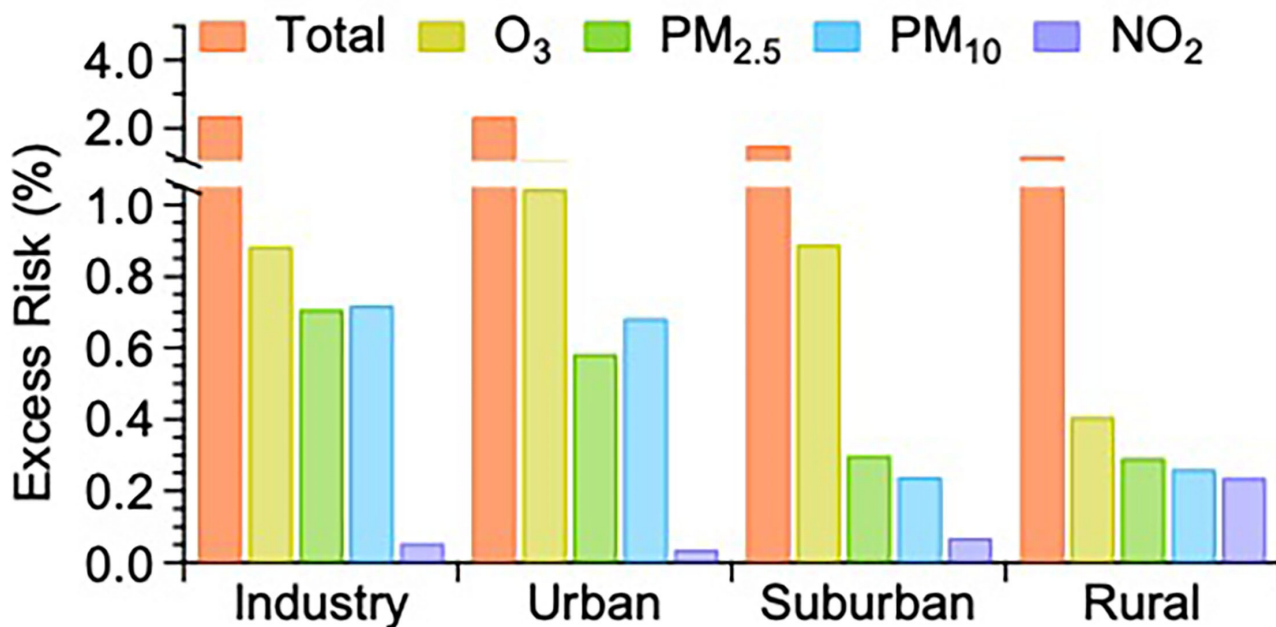


FIGURE 5  
The comparison of excess risks (ERs) averaged over 2017 and 2018 attributable to the sum and individual air pollutants among the four functional areas in Jinan.

and IA, the contribution rate of PM<sub>10</sub> decreased from 29.6 and 31.7% in 2017 to 19.5 and 23.6% in 2018, while PM<sub>2.5</sub> increased from 28.63 and 19.9% in 2017 to 31.2 and 36.2% in 2018,

respectively. In RA, the trend of PM<sub>10</sub> and PM<sub>2.5</sub> contributions to premature death was thus different to that in the other functional areas.

TABLE 1 Premature mortality attributable to short-term exposure to different air pollutants and their emission sources in 2017 and 2018, respectively.

Air pollutant	2017				2018			
	Premature death (person)	Urban	Contribution (%)		Premature death (person)	Urban	Contribution (%)	
		Suburban				Suburban		
		Rural				Rural		
		Industry				Industry		
NO <sub>2</sub>	<b>912</b>	17	<b>15.0</b>	1.53	<b>175</b>	9	<b>8.2</b>	1.7
		22		1.7		16		1.4
		392		22.9		34		7.2
		481		24.9		127		15.8
O <sub>3_8h</sub>	<b>1,755</b>	490	<b>28.9</b>	43.5	<b>666</b>	236	<b>31.0</b>	48.3
		522		40.1		175		47.8
		288		16.8		57		11.8
		456		23.6		198		24.5
PM <sub>10</sub>	<b>1,824</b>	298	<b>30.0</b>	26.4	<b>593</b>	147	<b>27.7</b>	30.1
		385		29.6		71		19.5
		528		30.9		184		38.2
		613		31.7		191		23.6
PM <sub>2.5</sub>	<b>1,581</b>	322	<b>26.0</b>	28.6	<b>710</b>	97	<b>33.1</b>	19.9
		373		28.6		114		31.2
		501		29.3		206		42.8
		386		19.9		292		36.2
Total	<b>6,072</b>	1,127	<b>100</b>	100	<b>2,145</b>	489	<b>100</b>	100
		1,301		100		366		100
		1,708		100		482		100
		1,936		100		808		100

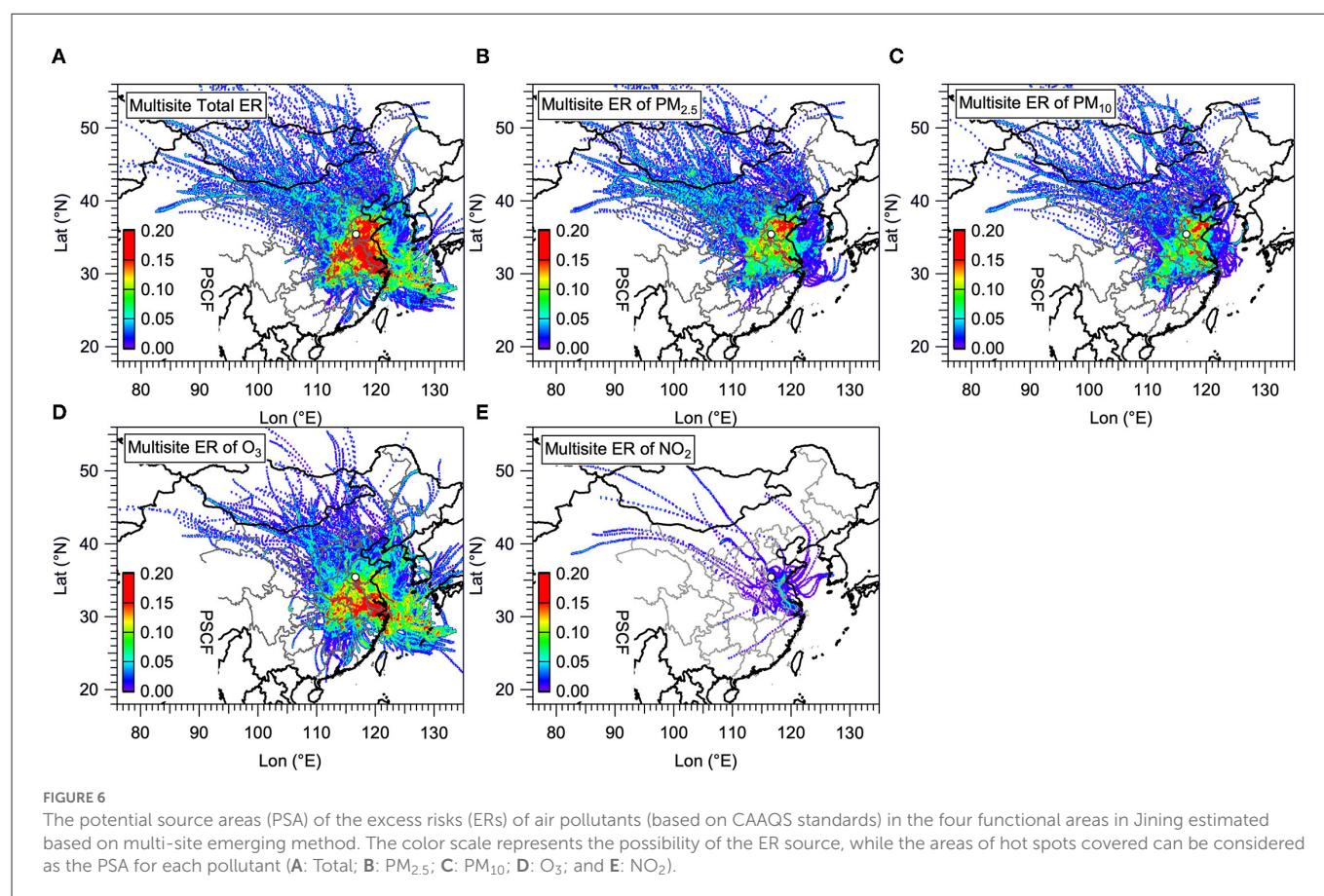
Bold indicate total numbers, rows beside each total from top to bottom are numbers for UA, SA, RA, and IA.

### 3.4. Identify the contributions of air pollutants to health risk

The PSCF analysis (see methods in section 2.4) was used to identify which functional areas and air pollutants are the major contributors to the health risk in Jining (Figure 6). To this end, the total ER in each functional area is first calculated by adding up the ER of all six pollutants according to Eq. 3, and then the multi-site merging method (see Eq. 17) was applied for calculating the multi-site ER for the total (Figure 6A) and PM<sub>2.5</sub> (Figure 6B), PM<sub>10</sub> (Figure 6C), O<sub>3</sub> (Figure 6D), and NO<sub>2</sub> (Figure 6E) contributions in Jining, respectively. In Figure 6, the color scale represents the possibility of the ER source, while the areas of hot spots covered can be considered as the Potential Source Areas (PSA) for each pollutant. The information obtained from this analysis is expected to offer important information to the local government in Jining on which air regulation measures to implement to reduce public exposure to health risks depending on the different functional areas.

For the total ER in Jining, the dominant PSA are mainly located in the north and central of Shandong Province, including Jining city itself, and also expand to significant fractions of the southeast of

Henan Province and the Anhui Province, and almost the total area of Yangtze River Delta (YRD). Besides, there was still a small part of PSA located in the northwest of Hubei Province and East China Sea extending from Henan Province and YRD, respectively. The hot spot areas in the north direction of ER for PM<sub>2.5</sub> was larger than that for PM<sub>10</sub>, thus ER for PM<sub>2.5</sub> was considered as the major contributor of the total ER in the north direction. In the south direction, the contribution to the PSA of the total ER is mostly attributable to O<sub>3</sub>, followed by that attributable to PM<sub>2.5</sub>, PM<sub>10</sub>, and NO<sub>2</sub>. After identifying the PSA of the total ER in different directions, we further calculated the Pearson coefficient (*r*) and Spearman coefficient (*s*) between the PSA for ER of each pollutant and that for the total ER (Figure 7). From the results of the two coefficients, the ER of O<sub>3</sub> (*r* of 0.86) had the tightest association with the total ER, followed by that of PM<sub>2.5</sub> (*r* of 0.76), PM<sub>10</sub> (*r* of 0.75), and NO<sub>2</sub> (*r* of 0.42) when just considering the *r*. The ER of NO<sub>2</sub>, on the other hand, was only weakly correlated with the total ER exhibiting the lowest *r* of 0.4 and *s* of 0.42. This finding stress that the local government in Jining should take urgent ways to reduce O<sub>3</sub> pollution as well as PM in the south direction and north direction of Jining City, respectively.



### 3.5. Effects of meteorological factors on health risk

Figure 8 shows the bivariate polar plots of HAQI in four functional areas during 2017 and 2018. In Figure 8, the horizontal (W-E) and vertical (S-N) axes represent the wind directions, the length of the radial contours represents the wind speed, and the color bar scale indicates HAQI values. HAQI varied depending on the wind speed and wind direction. The layout of Figures 8A–D is displayed according to the actual geographic location of each functional site in Jining. For instance, the UA (Figure 8C) and RA (Figure 8D) sites are located in the west and south of the IA (Figure 8B) site, respectively. The SA (Figure 8A) site is on the west side of the UA. When the wind speed was low in IA and RA, the HAQIs were both higher indicating a local source leading to the high HAQI values. It also reveals high HAQIs for wind directions from the southeast and southwest suggesting two potential transport directions in IA. The RA site also had two potential transport directions in the southwest and northwest. Conversely, when the windspeed was higher at the UA and SA sites, the HAQI resulted in higher values, suggesting high HAQIs at these two sites can be attributed to transport from nearby pollution sources in the northeast and southeast directions. From the analysis above, IA has been identified as a likely source for increased health risk in UA and SA in situations with east wind direction.

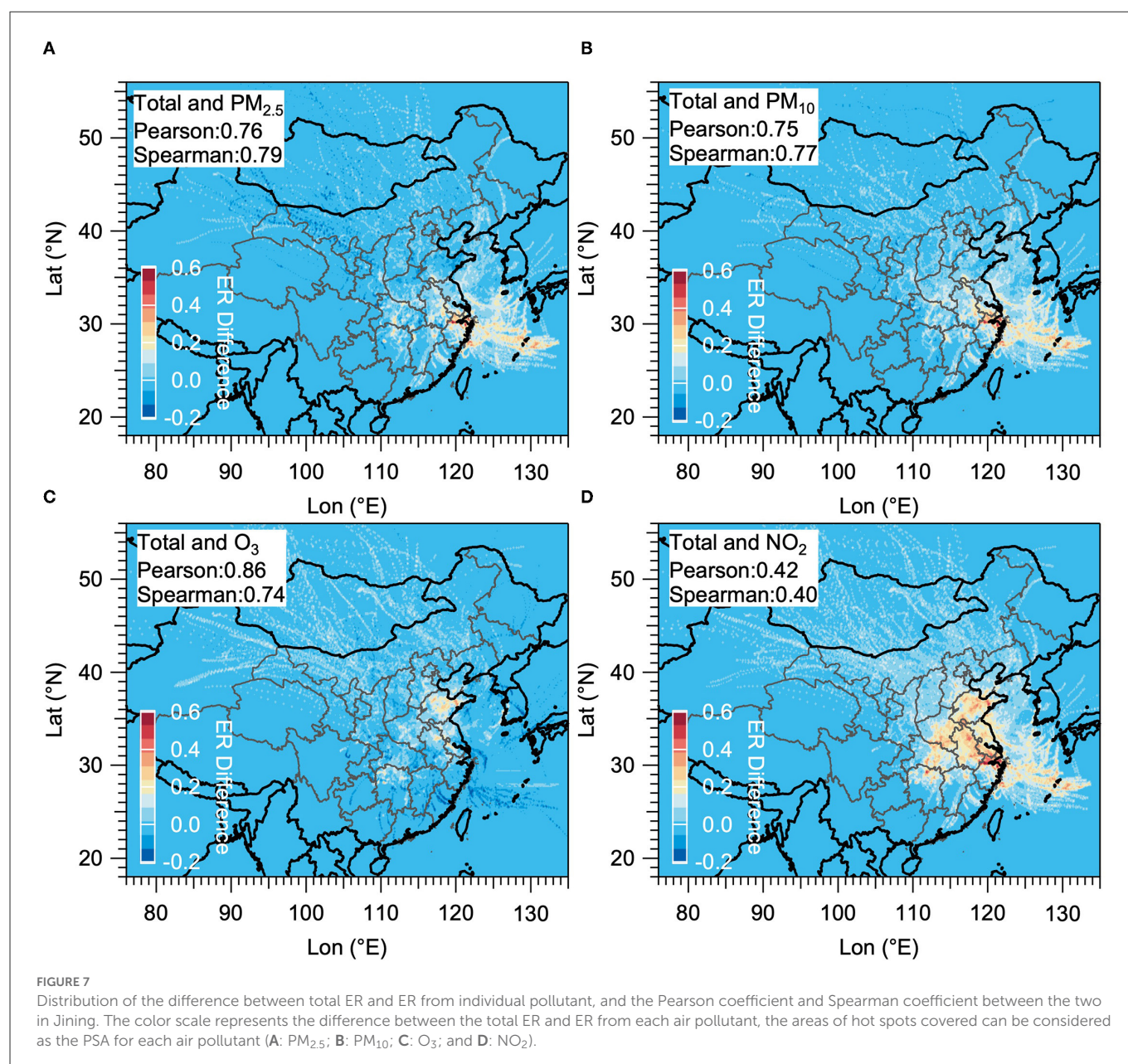
Figure 9 illustrates the HAQI variation depending on the temperature in IA, UA, SA and RA (Figure 5a–d). At each site, the triangles (HAQI in 2017) and circles (HAQI in 2018) indicate the distribution of HAQI events in each temperature bin, with the circle size depending on the ER values and the circle color indicating

the season during which the event occurred. Overall, in all four functional areas, more ER days (UA: 150, SA: 147, RA: 145, IA: 145) occurred in the temperature range of 25 to 30°C (that is primarily during summer), but higher averaged HAQI (UA: 134.7, SA: 140.28, RA: 139.66, IA: 149.24) presented in the temperature bin of 0 to 5°C (that is mostly during winter). High frequency of Ozone pollution days led to more ER days in summer, while less PM pollution days coupled with more severe pollution levels attributed to higher average HAQI in winter.

### 4. Policy implication

To better protect the public's health in Jining as well as in the whole of China, the local government should design certain policies and execute mitigation measures to tackle the threat to the public's health. Firstly, the multi-pollutant index should be considered when policymakers are developing relative regulations. Air quality standards are generally constructed based on the summary of the research evidence on the assessment of health impact attributable to each air pollutant separately. With the emergence of the multi-pollutant health index's framework and the increasing epidemiological evidence of the health effects, the future application of the multi-pollutant health index will become possible, even though there are still many uncertainties. Moreover, standards for multi-species air pollution levels should be built. If the multi-pollutant-oriented health risk assessment (including their statistical uncertainty) could be estimated with high reliability, then the air quality standards could be built on the base of the multi-species air





pollution level. For example, this study in Jining city found that PM<sub>10</sub> was the dominant contributor to premature mortality but the O<sub>3</sub> pollution level increased simultaneously. Thus, it would be better to define a standard for PM<sub>10</sub> that considers the ozone pollution level. Finally, if the pollution source that leads to health risks for the humans is identified, the mitigation regulations could be designed such that it would account for the relative importance of the primary and secondary pollutants. For example, in Jining city, the ozone pollution level increased from 2017 to 2018, and control measures should be taken that yield a more balanced control of the levels of VOC and NO<sub>x</sub>, which are the precursors of ozone.

## 5. Conclusion and remarks

In this study, four ambient air sampling sites in different functional areas, including urban, suburban, industrial, and rural areas, were selected to explore air pollution characteristics and the

exposure health risk to the public in Jining. The spatiotemporal distribution, exposure health risks, and potential source areas of each functional area were compared for 2017 and 2018 in Jining. Overall, all average air pollutant concentrations in Jining decreased between 2017 and 2018, except for O<sub>3</sub>, which showed an increase. The four functional areas showed the same seasonal and diurnal patterns among the six criteria air pollutants considered. The mass concentration of PM and NO<sub>2</sub> in IA and RA showed higher concentrations, respectively. The total premature deaths attributable to air pollution were 6,072 and 2,145 in 2017 and 2018 respectively, attributing to the decrease of air pollutants' concentrations and reflecting the benefits of controlling air pollution levels to human health in this region. Local pollutant emissions mainly contributed to high HAQI values in IA and RA, while high HAQI in UA and SA may instead be attributed to long-distance pollution transport. The ER of O<sub>3</sub> was with the highest  $r$ , reflecting the dominant contributor to the potential source area for total ER in the south, while PM was the main contributor to the potential source area

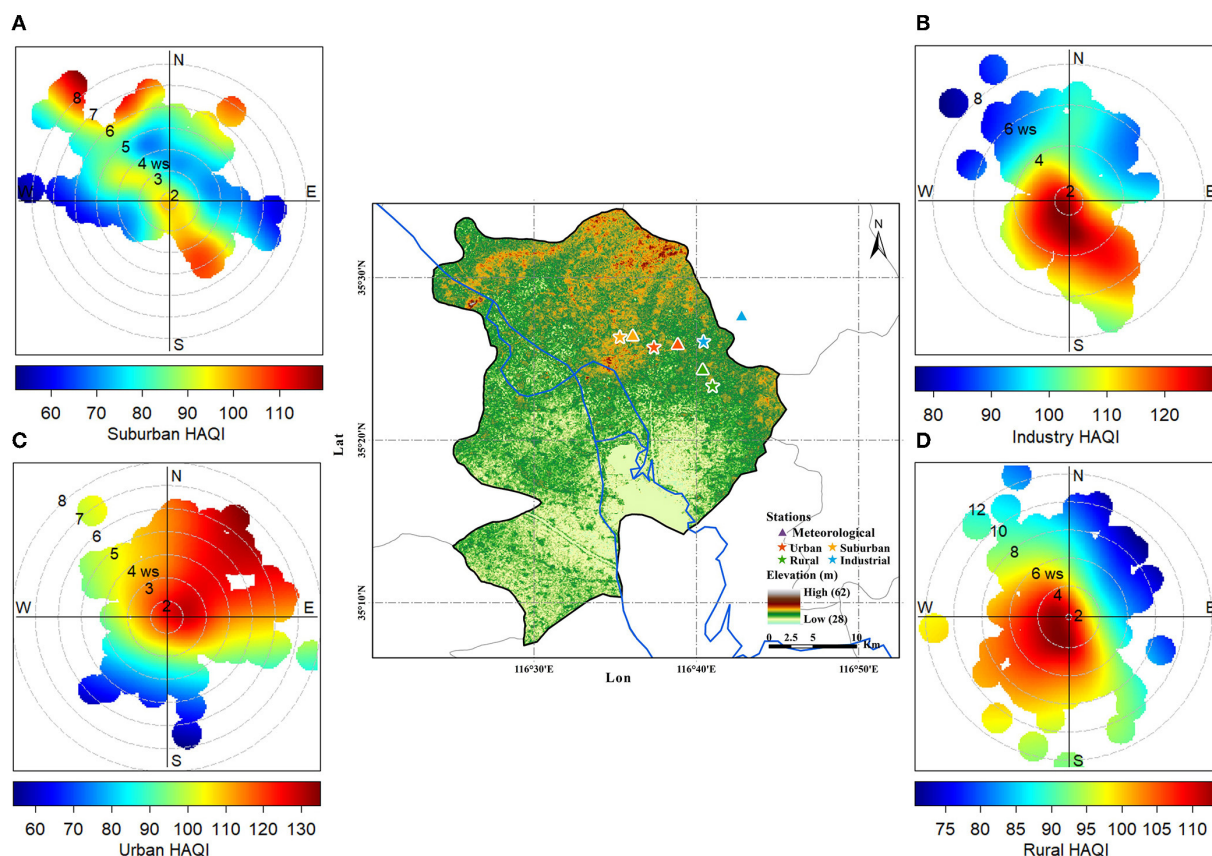


FIGURE 8

The bivariate polar plots of HAQI in suburban (A), industry (B), urban (C), and rural (D) areas in Jining. The horizontal (W–E) and vertical (S–N) axes in the bivariate polar plots represent the wind directions, the length of the radial contours represents the wind speed, and the color bar scale indicates HAQI values.

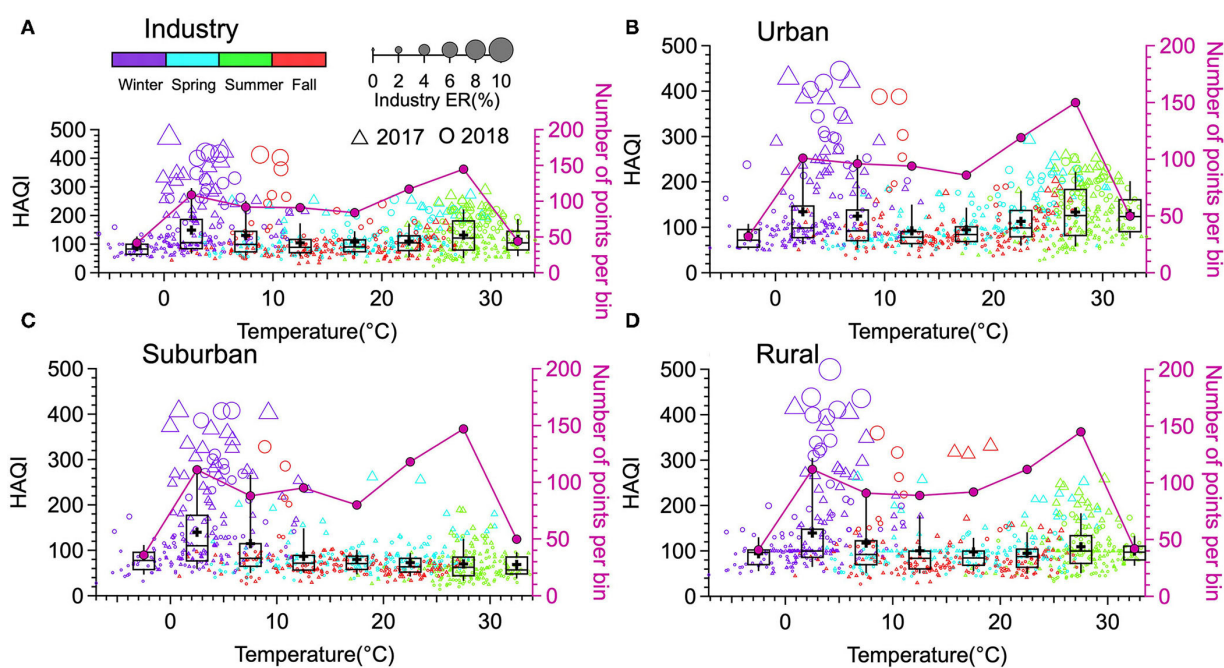


FIGURE 9

The HAQI variation depends on the temperature in the four functional areas (A: Industry; B: Urban; C: Suburban; D: Rural) in Jining. The triangles (HAQI in 2017) and circles (HAQI in 2018) indicate the distribution of HAQI events in each temperature bin, with the circle size depending on the ER values and the circle color indicating the season.



of total ER in the north. Overall, these results highlight that IA is the main local pollution source and that the most urgent measures should be taken to reduce O<sub>3</sub> pollution and particulate matter (PM), especially in industrial and urban areas to improve public health.

Results demonstrated in this study imply that O<sub>3</sub> rather than PM might become the primary threat to the public's health and urgent measures should be taken in the IA region in Jining city. However, it should be noted that this health assessment includes uncertainties due to various factors such as the ER calculation, measurement errors, and degree of correction between pollutants etc. More epidemiologic studies are required in the future to validate whether or not the HAQI is reliable to represent the multi-pollutant's health risk. Simultaneously, more attention should be paid on how to select the baseline concentration and ER coefficients since the results are sensitive to these measures as well.

## Data availability statement

The original contributions presented in the study are included in the article/[Supplementary material](#), further inquiries can be directed to the corresponding authors.

## Author contributions

YY: conceptualization, methodology, software, data curation, writing—original draft, software, and validation. XZ, JZ, DN, BW, LW, and MX: data curation. FS: conceptualization, methodology, software, writing—original draft, supervision, software, validation, and writing—review and editing. MH: conceptualization, methodology, supervision, software, validation, and writing—review and editing. All authors contributed to the article and approved the submitted version.

## References

- HEI. *State of Global Air 2020*. Boston, MA: Health Effects Institute (2020).
- Achakulwisut P, Brauer M, Hystad P, Anenberg SC. Global, national, and urban burdens of paediatric asthma incidence attributable to ambient NO<sub>2</sub> pollution: estimates from global datasets. *Lancet Planet Health*. (2019) 3:e166–78. doi: 10.1016/S2542-5196(19)30046-4
- Fu P, Guo X, Cheung FMH, Yung KKL. The association between PM<sub>2.5</sub> exposure and neurological disorders: a systematic review and meta-analysis. *Sci Tot Environ*. (2019) 655:1240–8. doi: 10.1016/j.scitotenv.2018.11.218
- Lelieveld J, Pozzer A, Pöschl U, Fnais M, Haines A, Münzel T. Loss of life expectancy from air pollution compared to other risk factors: a worldwide perspective. *Cardiovasc Res*. (2020) 116:1910–7. doi: 10.1093/cvr/cvaa025
- Shin J, Choi J, Kim KJ. Association between long-term exposure of ambient air pollutants and cardiometabolic diseases: a 2012 Korean Community Health Survey. *Nutr Metab Cardiovasc Dis*. (2019) 29:144–51. doi: 10.1016/j.numecd.2018.09.008
- Shou Y, Huang Y, Zhu X, Liu C, Hu Y, Wang H. A review of the possible associations between ambient PM<sub>2.5</sub> exposures and the development of Alzheimer's disease. *Ecotoxicol Environ Saf*. (2019) 174:344–52. doi: 10.1016/j.ecoenv.2019.02.086
- Yuan Y, Wu Y, Ge X, Nie D, Wang M, Zhou H, et al. *In vitro* toxicity evaluation of heavy metals in urban air particulate matter on human lung epithelial cells. *Sci Tot Environ*. (2019) 678:301–8. doi: 10.1016/j.scitotenv.2019.04.431
- Diao B, Ding L, Zhang Q, Na J, Cheng J. Impact of urbanization on PM<sub>2.5</sub>-related health and economic loss in China 338 cities. *Int J Environ Res Public Health*. (2020) 17:990. doi: 10.3390/ijerph17030990
- Sohrabi S, Zietsman J, Khreis H. Burden of disease assessment of ambient air pollution and premature mortality in urban areas: the role of socioeconomic status and transportation. *Int J Environ Res Public Health*. (2020) 17:1166. doi: 10.3390/ijerph17041166
- Wang Q, Wang J, He MZ, Kinney PL, Li T. A county-level estimate of PM<sub>2.5</sub> related chronic mortality risk in China based on multi-model exposure data. *Environ Int*. (2018) 110:105–12. doi: 10.1016/j.envint.2017.10.015
- Zhu G, Hu W, Liu Y, Cao J, Ma Z, Deng Y, et al. Health burdens of ambient PM<sub>2.5</sub> pollution across Chinese cities during 2006–2015. *J Environ Manag*. (2019) 243:250–6. doi: 10.1016/j.jenvman.2019.04.119
- Cibella F, Cuttitta G, Della Maggiore R, Ruggieri S, Panunzi S, et al. Effect of indoor nitrogen dioxide on lung function in urban environment. *Environ Res*. (2015) 138:8–16. doi: 10.1016/j.envres.2015.01.023
- Chen T-M, Kuschner WG, Gokhale J, Shofer S. Outdoor air pollution: nitrogen dioxide, sulfur dioxide, and carbon monoxide health effects. *Am J Med Sci*. (2007) 333:249–56. doi: 10.1097/MAJ.0b013e31803b900f

## Funding

This work was supported by the Meteorological Science and Technology Research Project of the Jining Meteorological Bureau (2019JNZL06 and 2022JNZL09) and Guided project of Shandong Meteorological Bureau (2021SDYD27).

## Acknowledgments

The authors gratefully acknowledge the Jining Meteorological Bureau for providing the air quality monitoring data and meteorological factor data.

## Conflict of interest

The authors declare that the research was conducted in the absence of any commercial or financial relationships that could be construed as a potential conflict of interest.

## Publisher's note

All claims expressed in this article are solely those of the authors and do not necessarily represent those of their affiliated organizations, or those of the publisher, the editors and the reviewers. Any product that may be evaluated in this article, or claim that may be made by its manufacturer, is not guaranteed or endorsed by the publisher.

## Supplementary material

The Supplementary Material for this article can be found online at: <https://www.frontiersin.org/articles/10.3389/fpubh.2023.1075262/full#supplementary-material>

14. Kim CS, Alexis NE, Rappold AG, Kehrl H, Hazucha MJ, Lay JC, et al. Lung function and inflammatory responses in healthy young adults exposed to 0.06 ppm ozone for 6.6 hours. *Am J Respir Crit Care Med*. (2011) 183:1215–21. doi: 10.1164/rccm.201111-1813OC
15. Kim J, Han Y, Seo SC, Lee JY, Choi J, Kim KH, et al. Association of carbon monoxide levels with allergic diseases in children. *Allergy Asthma Proc*. (2016) 37:e1–7. doi: 10.2500/aap.2016.37.3918
16. Jiang Y, Niu Y, Xia Y, Liu C, Lin Z, Wang W, et al. Effects of personal nitrogen dioxide exposure on airway inflammation and lung function. *Environ Res*. (2019) 177:108620. doi: 10.1016/j.envres.2019.108620
17. Goudarzi G, Geravandi S, Idani E, Hosseini SA, Baneshi MM, Yari AR, et al. An evaluation of hospital admission respiratory disease attributed to sulfur dioxide ambient concentration in Ahvaz from 2011 through 2013. *Environ Sci Pollut Res*. (2016) 23:22001–7. doi: 10.1007/s11356-016-7447-x
18. Nuvolone D, Petri D, Voller F. The effects of ozone on human health. *Environ Sci Pollut Res*. (2018) 25:8074–88. doi: 10.1007/s11356-017-9239-3
19. Kim K-H, Jahan SA, Kabir E. A review on human health perspective of air pollution with respect to allergies and asthma. *Environ Int*. (2013) 59:41–52. doi: 10.1016/j.envint.2013.05.007
20. Krzyzanowski M, Cohen A, Anderson R. Quantification of health effects of exposure to air pollution. *Occup Environ Med*. (2002) 59:791. doi: 10.1136/oem.59.12.791
21. Luo H, Guan Q, Lin J, Wang Q, Yang L, Tan Z, et al. Air pollution characteristics and human health risks in key cities of northwest China. *J Environ Manage*. (2020) 269:110791. doi: 10.1016/j.jenvman.2020.110791
22. Maji KJ, Dikshit AK, Arora M, Deshpande A. Estimating premature mortality attributable to PM<sub>2.5</sub> exposure and benefit of air pollution control policies in China for 2020. *Sci Tot Environ*. (2018) 612:683–93. doi: 10.1016/j.scitotenv.2017.08.254
23. Hu J, Huang L, Chen M, Liao H, Zhang H, Wang S, et al. Premature mortality attributable to particulate matter in china: source contributions and responses to reductions. *Environ Sci Technol*. (2017) 51:9950–9. doi: 10.1021/acs.est.7b03193
24. Shaddick G, Thomas ML, Mudu P, Ruggeri G, Gumy S. Half the world's population are exposed to increasing air pollution. *NPJ Clim Atmos Sci*. (2020) 3:23. doi: 10.1038/s41612-020-0124-2
25. Chowdhury S, Pozzer A, Haines A, Klingmüller K, Münzel T, Paasonen P, et al. Global health burden of ambient PM<sub>2.5</sub> and the contribution of anthropogenic black carbon and organic aerosols. *Environ Int*. (2022) 159:107020. doi: 10.1016/j.envint.2021.107020
26. Maji KJ, Namdeo A. Continuous increases of surface ozone and associated premature mortality growth in China during 2015–2019. *Environ Pollut*. (2021) 269:116183. doi: 10.1016/j.envpol.2020.116183
27. Wang C, Wang Y, Shi Z, Sun J, Gong K, Li J, et al. Effects of using different exposure data to estimate changes in premature mortality attributable to PM<sub>2.5</sub> and O<sub>3</sub> in China. *Environ Pollut*. (2021) 285:117242. doi: 10.1016/j.envpol.2021.117242
28. Kan H, Chen R, Tong S. Ambient air pollution, climate change, and population health in China. *Environ Int*. (2012) 42:10–9. doi: 10.1016/j.envint.2011.03.003
29. Chen R, Samoli E, Wong C-M, Huang W, Wang Z, Chen B, et al. Associations between short-term exposure to nitrogen dioxide and mortality in 17 Chinese cities: the China Air Pollution and Health Effects Study (CAHES). *Environ Int*. (2012) 45:32–8. doi: 10.1016/j.envint.2012.04.008
30. Chen R, Pan G, Zhang Y, Xu Q, Zeng G, Xu X, et al. Ambient carbon monoxide and daily mortality in three Chinese cities: the China Air Pollution and Health Effects Study (CAHES). *Sci Tot Environ*. (2011) 409:4923–8. doi: 10.1016/j.scitotenv.2011.08.029
31. Chen R, Huang W, Wong C-M, Wang Z, Thach TQ, Chen B, et al. Short-term exposure to sulfur dioxide and daily mortality in 17 Chinese cities: the China air pollution and health effects study (CAHES). *Environ Res*. (2012) 118:101–6. doi: 10.1016/j.envres.2012.07.003
32. Wu R, Zhong L, Huang X, Xu H, Liu S, Feng B, et al. Temporal variations in ambient particulate matter reduction associated short-term mortality risks in Guangzhou, China: a time-series analysis (2006–2016). *Sci Tot Environ*. (2018) 645:491–8. doi: 10.1016/j.scitotenv.2018.07.091
33. Chen C, Xu D, He MZ, Wang Y, Du Z, Du Y, et al. Fine particle constituents and mortality: a time-series study in Beijing, China. *Environ Sci Technol*. (2018) 52:11378–86. doi: 10.1021/acs.est.8b00424
34. Yang C, Yang H, Guo S, Wang Z, Xu X, Duan X, et al. Alternative ozone metrics and daily mortality in Suzhou: the China Air Pollution and Health Effects Study (CAHES). *Sci Tot Environ*. (2012) 426:83–9. doi: 10.1016/j.scitotenv.2012.03.036
35. Dominici F, Peng RD, Barr CD, Bell ML. Protecting human health from air pollution: shifting from a single-pollutant to a multi-pollutant approach. *Epidemiology*. (2010) 21:187. doi: 10.1097/EDE.0b013e3181cc86e8
36. Zhu Y, Wang Y, Xu H, Luo B, Zhang W, Guo B, et al. Joint effect of multiple air pollutants on daily emergency department visits in Chengdu, China. *Environ Pollut*. (2020) 257:113548. doi: 10.1016/j.envpol.2019.113548
37. Shen F, Ge X, Hu J, Nie D, Tian L, Chen M. Air pollution characteristics and health risks in Henan Province, China. *Environ Res*. (2017) 156:625–34. doi: 10.1016/j.envres.2017.04.026
38. Swamee PK, Tyagi A. Formation of an air pollution index. *J Air Waste Manag Assoc*. (1999) 49:88–91. doi: 10.1080/10473289.1999.10463776
39. Stieb DM, Burnett RT, Smith-Doiron M, Brion O, Shin HH, Economou V. A new multipollutant, no-threshold air quality health index based on short-term associations observed in daily time-series analyses. *J Air Waste Manag Assoc*. (2008) 58:435–50. doi: 10.3155/1047-3289.58.3.435
40. Hu J, Ying Q, Wang Y, Zhang H. Characterizing multi-pollutant air pollution in China: comparison of three air quality indices. *Environ Int*. (2015) 84:17–25. doi: 10.1016/j.envint.2015.06.014
41. Shen F, Zhang L, Jiang L, Tang M, Gai X, Chen M, et al. Temporal variations of six ambient criteria air pollutants from 2015 to 2018, their spatial distributions, health risks and relationships with socioeconomic factors during 2018 in China. *Environ Int*. (2020) 137:105556. doi: 10.1016/j.envint.2020.105556
42. Zhou W, Chen C, Lei L, Fu P, Sun Y. Temporal variations and spatial distributions of gaseous and particulate air pollutants and their health risks during 2015–2019 in China. *Environ Pollut*. (2021) 272:116031. doi: 10.1016/j.envpol.2020.116031
43. Biegalski S, Hopke P. Total potential source contribution function analysis of trace elements determined in aerosol samples collected near Lake Huron. *Environ Sci Technol*. (2004) 38:4276–84. doi: 10.1021/es035196s
44. Boichu M, Favez O, Riffault Y, Petit JE, Zhang Y, Brogniez C, et al. Large-scale particulate air pollution and chemical fingerprint of volcanic sulfate aerosols from the 2014–2015 Holuhraun flood lava eruption of Bárðarbunga volcano (Iceland). *Atmos Chem Phys*. (2019) 19:14253–87. doi: 10.5194/acp-19-14253-2019
45. Liu H, Liu C, Xie Z, Li Y, Huang X, Wang S, et al. A paradox for air pollution controlling in China revealed by “APEC Blue” and “Parade Blue”. *Sci Rep*. (2016) 6:34408. doi: 10.1038/srep34408
46. Zhao N, Wang G, Li G, Lang J, Zhang H. Air pollution episodes during the COVID-19 outbreak in the Beijing–Tianjin–Hebei region of China: an insight into the transport pathways and source distribution. *Environ Pollut*. (2020) 267:115617. doi: 10.1016/j.envpol.2020.115617
47. Dimitriou K, Grivas G, Liakakou E, Gerasopoulos E, Mihalopoulos N. Assessing the contribution of regional sources to urban air pollution by applying 3D-PSCF modeling. *Atmos Res*. (2021) 248:105187. doi: 10.1016/j.atmosres.2020.105187
48. Guo H, Huang S, Chen M. Air pollutants and asthma patient visits: indication of source influence. *Sci Tot Environ*. (2018) 625:355–62. doi: 10.1016/j.scitotenv.2017.12.298
49. Zhang L, Shen F, Gao J, Cui S, Yue H, Wang J, et al. Characteristics and potential sources of black carbon particles in suburban Nanjing, China. *Atmos Pollut Res*. (2020) 11:981–91. doi: 10.1016/j.apr.2020.02.011
50. Shang Y, Sun Z, Cao J, Wang X, Zhong L, Bi X, et al. Systematic review of Chinese studies of short-term exposure to air pollution and daily mortality. *Environ Int*. (2013) 54:100–11. doi: 10.1016/j.envint.2013.01.010
51. Nie D, Shen F, Wang J, Ma X, Li Z, Ge P, et al. Changes of air quality and its associated health and economic burden in 31 provincial capital cities in China during COVID-19 pandemic. *Atmos Res*. (2021) 249:105328. doi: 10.1016/j.atmosres.2020.105328
52. Tian X, Dai H, Geng Y, Wilson J, Wu R, Xie Y, Hao H. Economic impacts from PM<sub>2.5</sub> pollution-related health effects in China's road transport sector: a provincial-level analysis. *Environ Int*. (2018) 115:220–9. doi: 10.1016/j.envint.2018.03.030
53. Draxler R, Stunder B, Rolph G, Stein A, Taylor A. *HYSPLIT4 User's Guide, Version 4, Report*. Silver Spring, MD: NOAA (2012).
54. Polissar AV, Hopke PK, Paatero P, Kaufmann YJ, Hall DK, Bodhaine BA, et al. The aerosol at Barrow, Alaska: long-term trends and source locations. *Atmos Environ*. (1999) 33:2441–58. doi: 10.1016/S1352-2310(98)00423-3
55. Petit JE, Favez O, Albinet A, Canonaco F. A user-friendly tool for comprehensive evaluation of the geographical origins of atmospheric pollution: wind and trajectory analyses. *Environ Model Softw*. (2017) 88:183–7. doi: 10.1016/j.envsoft.2016.11.022
56. Wang F, Qiu X, Cao J, Peng L, Zhang N, Yan Y, et al. Policy-driven changes in the health risk of PM<sub>2.5</sub> and O<sub>3</sub> exposure in China during 2013–2018. *Sci Tot Environ*. (2021) 757:143775. doi: 10.1016/j.scitotenv.2020.143775
57. Wu J, Zhang Y, Wang T, Qian Y. Rapid improvement in air quality due to aerosol-pollution control during 2012–2018: an evidence observed in Kunshan in the Yangtze River Delta, China. *Atmos Pollut Res*. (2020) 11:693–701. doi: 10.1016/j.apr.2019.12.020
58. Xiao K, Wang Y, Wu G, Fu B, Zhu Y. Spatiotemporal characteristics of air pollutants (PM<sub>10</sub>, PM<sub>2.5</sub>, SO<sub>2</sub>, NO<sub>2</sub>, O<sub>3</sub>, and CO) in the Inland Basin City of Chengdu, Southwest China. *Atmosphere*. (2018) 9:74. doi: 10.3390/atmos9020074
59. Zhao S, Yin D, Yu Y, Kang S, Qin D, Dong L. PM<sub>2.5</sub> and O<sub>3</sub> pollution during 2015–2019 over 367 Chinese cities: SPATIOTEMPORAL variations, meteorological and topographical impacts. *Environ Pollut*. (2020) 264:114694. doi: 10.1016/j.envpol.2020.114694
60. Zheng S, Schlink U, Ho KF, Singh RP, Pozzer A. Spatial distribution of PM<sub>2.5</sub>-related premature mortality in China. *GeoHealth*. (2021) 5:e2021GH000532. doi: 10.1029/2021GH000532